JOC Article
pubs.acs.org/joc

Photophysics and Photodeprotection Reactions of *p*-Methoxyphenacyl Phototriggers: An Ultrafast and Nanosecond Time-Resolved Spectroscopic and Density Functional Theory Study

Hui-Ying An,[†] Wai Ming Kwok,[‡] Chensheng Ma,[†] Xiangguo Guan,[†] Jovi Tze Wai Kan,[†] Patrick H. Toy,[†] and David Lee Phillips*[,†]

[†]*Department of Chemistry, The University of Hong Kong, Pokfulam Road, Hong Kong S. A. R., P. R. China, and* [‡]*Department of Applied Biology and Chemical Technology, The Hong Kong Polytechnic University, Hung Hom, Kowloon, Hong Kong S. A. R., P. R. China*

phillips@hkucc.hku.hk

Received April 30, 2010

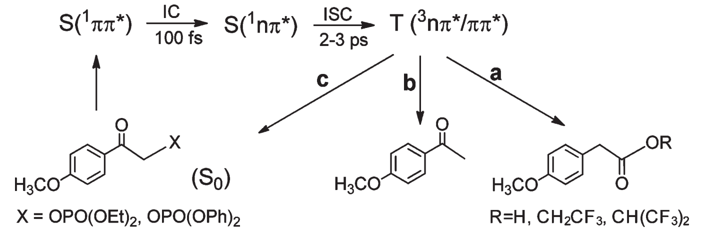

Time-resolved spectroscopic experiments were performed to investigate the kinetics and mechanisms of the photodeprotection reactions for *p*-methoxyphenacyl (*p*MP) compounds, *p*-methoxyphenacyl diethyl phosphate (MPEP) and diphenyl phosphate (MPPP). The experimental results reveal that compared to the previous reports for the counterpart *p*-hydroxyphenacyl (*p*HP) phosphates, the $^3n\pi^*/\pi\pi^*$ mixed character triplet of *p*MP acts as a reactive precursor that leads to the subsequent solvent and leaving group dependent chemical reactions and further affects the formation of photoproducts. The MPPP triplet in H_2O/CH_3CN and in fluorinated alcohols shows a rapid heterolytic cleavage ($\tau \approx 5.4$ ns) that results in deprotection and formation of a solvolytic rearrangement product, whereas the MPPP triplet in CH_3CN and the MPEP triplet in CH_3CN and H_2O/CH_3CN and fluorinated alcohols decay on a much longer time scale ($\tau \approx 100$ ns) with little observation of the rearrangement product. The density functional theory (DFT) calculations reveal a substantial solvation effect that is connected with the methoxy versus hydroxyl substitution in accounting for the different deprotection reactivity of *p*MP and *p*HP compounds. The results reported here provide new insight in elucidating the solvent and leaving group dependent dual reactivity of *p*MP compounds on the formation of the rearrangement versus reductive photoproduct.

Introduction

Several kinds of α-keto groups, especially those based on phenacyl groups, have received a great deal of attention due to their favorable properties for potential use as photochemically removable protecting groups (PRPGs) for the rapid release of various biological effectors.[1] Among the wide variety of phenacyl based PRPGs that have been examined in the literature, *para*-substituted phenacyls bearing the oxygen-containing electron donors of the *p*-hydroxyphenacyl (*p*HP) and *p*-methoxyphenacyl (*p*MP) groups were found to be particularly attractive due to their desirable ability in providing a very fast photodeprotection and the accompanying formation of biologically benign rearrangement byproducts.[1a,2] As a result, *p*HP compounds have been developed as an efficient "cage" for the

---

(1) (a) Givens, R. S.; Park, C. H. *Tetrahedron Lett.* **1996**, *37*, 6259–6262. (b) Givens, R. S.; Jung, A.; Park, C. H.; Weber, J.; Bartlett, W. *J. Am. Chem. Soc.* **1997**, *119*, 8369–8370.

(2) (a) Anderson, J. C.; Reese, C. B. *Tetrahedron Lett.* **1962**, *3*, 1–4. (b) Epstein, W. W.; Garrossian, M. *J. Chem. Soc., Chem. Commun.* **1987**, 532–533. (c) Baldwin, J. E.; Mcconnaughie, A. W.; Moloney, M. G.; Pratt, A. J.; Shim, S. B. *Tetrahedron* **1990**, *46*, 6879–6884. (d) Park, C. H.; Givens, R. S. *J. Am. Chem. Soc.* **1997**, *119*, 2453–2463. (e) Banerjee, A.; Lee, K.; Falvey, D. E. *Tetrahedron* **1999**, *55*, 12699–12710. (f) Zhang, K.; Corrie, J. E. T.; Munasinghe, V. R. N.; Wan, P. *J. Am. Chem. Soc.* **1999**, *121*, 5625–5632. (g) Conrad, P. G.; Givens, R. S.; Hellrung, B.; Rajesh, C. S.; Ramseier, M.; Wirz, J. *J. Am. Chem. Soc.* **2000**, *122*, 9346–9347. (h) Givens, R. S.; Weber, J. F. W.; Conrad, P. G.; Orosz, G.; Donahue, S. L.; Thayer, S. A. *J. Am. Chem. Soc.* **2000**, *122*, 2687–2697. (i) Specht, A.; Loudwig, S.; Peng, L.; Goeldner, M. *Tetrahedron Lett.* **2002**, *43*, 8947–8950.

DOI: 10.1021/jo100848b

liberation of a number of biological stimulants.[1,2d,h,3] Previous investigations on *p*HP and *p*MP compounds observed that the photochemistry of these two PRPGs is highly sensitive to solvent properties. The photodeprotection reaction of *p*HP caged compounds (eqs 1 and 2) occurs as the primary process in aqueous or largely aqueous solvents but does not take place noticeably in neat organic solvents such as acetonitrile (CH_3CN).[1,2d,f−h,3b,4] Our previous mechanistic studies utilizing direct time-resolved spectroscopic methods and indirect steady state quenching methods have presented explicit and consistent evidence indicating a direct triplet cleavage pathway for *p*HP photodeprotection.[5] Ultrafast experiments on a series of *p*HP caged phosphates and carboxylates (eq 2) in a H_2O/CH_3CN (1:1, v/v) solvent have found a stepwise water-assisted triplet deprotection-rearrangement pathway with the deprotection rate depending on the lability of the leaving group and ranging from $\sim 7 \times 10^9\ s^{-1}$ for HPPP (X = $OPO(OPh)_2$) to $\sim 2 \times 10^8\ s^{-1}$ for HPH (X = $OCO(CH_2)_5CH_3$).[5]

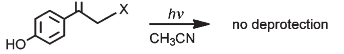

(1)

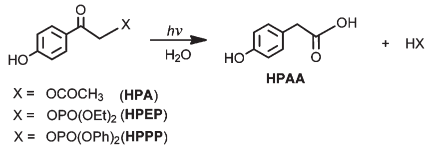

(2)

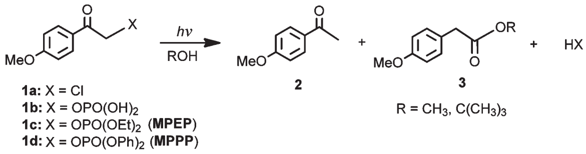

(3)

Unlike the relatively simple solvent dependence and cleanness of the product distribution displayed by the *p*HP phototriggers, photodeprotection of *p*MP caged compounds exhibits a more complicated solvent dependence and results in a more complex product distribution with a relatively low efficiency for deprotection.[2a−d,f,4,6] For example, it was reported that the photolysis of *p*MP dihydrogen phosphate (**1b**), *p*MP diethyl phosphate (MPEP, **1c**), and *p*MP diphenyl phosphate (MPPP, **1d**) in the hydrogen-donating solvent dioxane leads to deprotection along with the reduction product *p*-methoxyacetophenone (**2**) as the sole ketone byproduct.[2b,c] Different from this, photodeprotection of MPEP (**1c**)[6a,b] and *p*MP chloride (**1a**)[2a] in the less hydrogen-donating solvents of methanol, ethanol, or *tert*-butyl alcohol produces the corresponding rearranged esters *p*-methoxyphenylacetates (**3**) as the major byproduct and a minor amount of **2**. These observations suggest a solvent dependent *dual* reactivity of photoexcited *p*MP in giving two competing deprotection pathways that lead to, respectively, the reduction (**2**) and rearrangement (**3**) byproducts. The reduction accompanied *p*MP photorelease parallels the photodeprotection reaction reported for nonsubstituted phenacyl esters and electron-withdrawing substituted *p*-phenacyl chlorides.[2a] A laser flash photolysis (LFP) study by Falvey and co-workers found that such reactions of the nonsubstituted phenacyl PRPG arises from a very fast hydrogen abstraction (rate of $\sim 9 \times 10^6\ M^{-1}\ s^{-1}$) of the phenacyl triplet from the surrounding solvent.[7] The prevalence of the *p*MP reduction product (**2**) in solvents with better hydrogen-donating capacity as well as the relevant solvent isotope effects implies a primary role of the analogous hydrogen abstraction and associated reaction (denoted as "photoreduction" hereafter) in accounting for the observed *p*MP photodeprotection in these solvents.

In contrast to the knowledge determined for the *p*MP photoreduction, little is known about the nature of the major photochemical steps and key environmental factors accounting for the more biologically important *p*MP rearrangement reaction. It is relevant to note that a photochemistry study of MPEP shows its quantum efficiency in methanol is about only half of that of its *p*HP counterpart HPEP;[6a] in addition, *p*MP acetate was found to have low reactivity in a H_2O/CH_3CN (1:1, v/v) solvent, in sharp contrast to the efficient photorelease reaction of the corresponding HPA observed under the same experimental conditions.[1,2d,f−h,3b,4] As the *p*HP and *p*MP cages apparently have similar configurations, the substantially different photochemistry and reactivity of the corresponding phototriggers may suggest a crucial effect associated with replacing the hydroxy group in *p*HP by the methoxy group in *p*MP. Up to now, the relevant photophysics and photochemistry of *p*MP have remained little understood, and the underlying cause of this substitution effect has not been investigated in great detail to the best of our knowledge. Such information is, however, important in terms of understanding the mechanism of *p*MP deprotection as well as helping to clarify some uncertainty in the *p*HP rearrangement reaction. The *p*HP versus *p*MP substitution effect and the complex solvent and leaving group sensitive *p*MP reactivity toward the deprotection and the competitive hydrogen absorption is an interesting example of the widely known substituent and solvent dependent photoreactivity of the general family of aromatic carbonyl compounds. In this sense, *p*MP compounds offer a good exemplar to explore this ubiquitous but not fully understood substituent and solvent dependent photoreactivity phenomenon in phenacyl type aromatic carbonyl compounds.

As an extension of our previous work on various *p*HP phototriggers,[5] we have conducted a combined femtosecond time-resolved fluorescence (fs-TRF), femtosecond transient absorption (fs-TA), and picosecond and nanosecond time-resolved Raman (ps-, ns-TR^3) study on two synthesized *p*MP compounds, MPEP and MPPP, in a range of solvents including neat CH_3CN, H_2O/CH_3CN (1:1, v/v), CF_3CH_2OH, and $CF_3CHOHCF_3$ with the aim of helping to address the issues mentioned in the preceding paragraph. DFT calculations were performed to help map the reaction pathways and locate transient states and reaction barriers for the *p*MP deprotection reaction in water-containing solvents. These experimental and computational results taken together suggest a mechanism where solvation of the leaving group initiates a triplet liberation and rearrangement pathway for the *p*MP photodeprotection. The data provide explicit dynamic information and a mechanistic

---

(3) (a) Gee, K. R.; Kueper, L. W.; Barnes, J.; Dudley, G.; Givens, R. S. *J. Org. Chem.* **1996**, *61*, 1228–1233. (b) Conrad, P. G.; Givens, R. S.; Weber, J. F. W.; Kandler, K. *Org. Lett.* **2000**, *2*, 1545–1547.

(4) Brousmiche, D. W.; Wan, P. *J. Photochem. Photobiol., A* **2000**, *130*, 113–118.

(5) (a) Ma, C. S.; Kwok, W. M.; Chan, W. S.; Zuo, P.; Kan, J. T. W.; Toy, P. H.; Phillips, D. L. *J. Am. Chem. Soc.* **2005**, *127*, 1463–1472. (b) Ma, C. S.; Kwok, W. M.; Chan, W. S.; Du, Y.; Kan, J. T. W.; Toy, P. H.; Phillips, D. L. *J. Am. Chem. Soc.* **2006**, *128*, 2558–2570.

(6) (a) Givens, R. S.; Athey, P. S.; Matuszewski, B.; Kueper, L. W.; Xue, J. Y.; Fister, T. *J. Am. Chem. Soc.* **1993**, *115*, 6001–6012. (b) Givens, R. S.; Kueper, L. W. *Chem. Rev.* **1993**, *93*, 55–66. (c) Sheehan, J. C.; Umezawa, K. *J. Org. Chem.* **1973**, *38*, 3771–3774.

(7) Banerjee, A.; Falvey, D. E. *J. Am. Chem. Soc.* **1998**, *120*, 2965–2966.

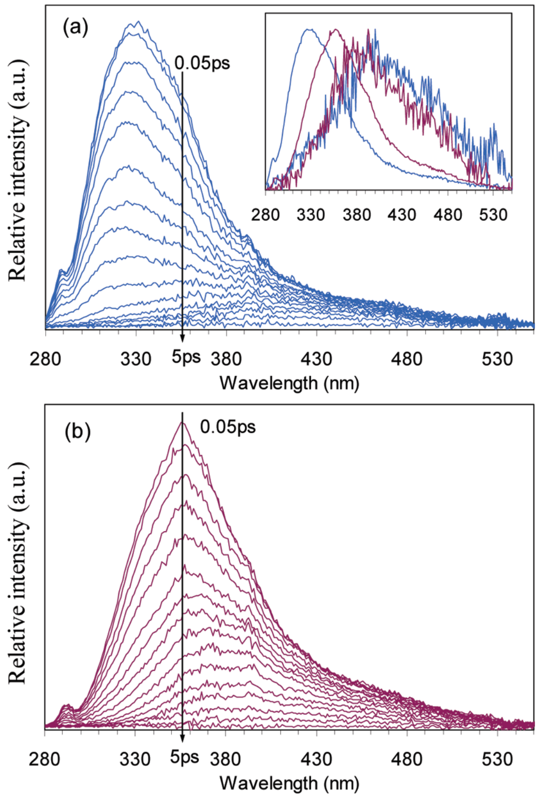

FIGURE 1. Fs-TRF spectra of MPEP obtained with 267 nm excitation in (a) CH_3CN and (b) H_2O/CH_3CN (1:1, v/v). The arrows indicate the spectral evolution in the two solvents. The inset in panel a shows a comparison of the normalized fluorescence spectra at 0.05 ps (λ_{max} at 330–360 nm) and 1.2 ps ((λ_{max} at 400–420 nm) in CH_3CN (blue) and H_2O/CH_3CN (purple).

description for each of the steps involved in the overall reaction scheme of the *p*MP photodeprotection. In addition, since the hydroxyl proton involved excited-state processes that may occur in the *p*HP deprotection are unlikely to be included in the *p*MP photodeprotection, a direct comparison of the dynamics and reaction pathways obtained here for the *p*MP phosphates with those reported for the counterpart *p*HP phosphates will provide direct evidence for identifying the particular excited state step(s) that associate(s) with the effect of methoxy versus hydroxyl substitution. This will in turn help to reveal the molecular origin of the different deprotection photochemistry displayed by the *p*MP and *p*HP phototriggers.

Results and Discussion

Femtosecond Time-Resolved Fluorescence (fs-TRF) Spectroscopy. Comparative fs-TRF measurements were done for the compounds in CH_3CN and H_2O/CH_3CN to characterize the spectral properties, dynamics, and the effect of water on the singlet character excited state(s) populated by the 267 nm photoexcitation. Representative spectra recorded for MPEP in the two solvents are displayed in Figure 1a and b, respectively. In both of the solvents, the TRF spectra display a similar very rapid decay from an initial relatively strong fluorescence (profiles of this fluorescence have λ_{max} at ~330 nm in CH_3CN and ~360 nm in H_2O/CH_3CN) into a rather weak and red-shifted fluorescence band with the λ_{max} at ~420 and ~400 nm in the respective solvents followed by a quick decay of the latter on a few picoseconds time scale. As a result of this, the time profile of the fluorescence intensity varies significantly and exhibits an increasingly slower decay dynamics as the fluorescence wavelength increases. Figure 2 shows the time dependences of the fluorescence intensity at three selected wavelengths and the associated exponential fitting results obtained from simulation of the experimental data containing a convolution of the instrumental response function (IRF). This fitting found that the wavelength dependent decay dynamics in the two solvents can both be described satisfactorily by similar sets of two time constants of ~0.1 and ~1.0 ps for those in CH_3CN and ~0.1 and ~1.3 ps in H_2O/CH_3CN. The traces at different wavelengths shown in Figure 2 were fit to an instrumental response function (IRF) convolved two exponential fittings to the experimental data. The trace at 330 nm in Figure 2 has mainly a large contribution from the shorter lived species responsible for the fluorescence with λ_{max} at ~330 nm in CH_3CN and ~360 nm in H_2O/CH_3CN and hence has a faster decay, while the trace at 450 nm in Figure 2 mainly has contributions from the longer lived species responsible for the fluorescence band with the λ_{max} at ~420 and ~400 nm in the respective solvents and thus has a comparatively longer decay at this wavelength.

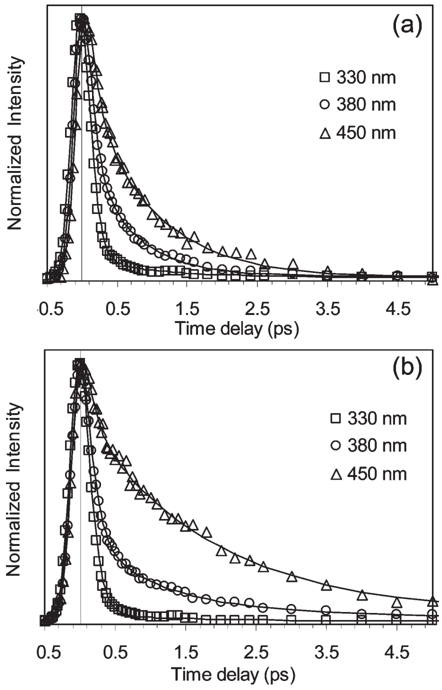

FIGURE 2. Normalized fluorescence decay profiles of MPEP at the labeled fluorescence wavelengths observed with the 267 nm excitation in (a) CH_3CN and (b) H_2O/CH_3CN (1:1, v/v) are shown. The solid lines show the instrumental response function (IRF) convolved two exponential fittings to the experimental data.

It is known that, for typical substituted aromatic carbonyl systems including the *p*MP chromophore (e.g., the spectra at $t = 0$ in Figure 1S in the Supporting Information), the longest wavelength absorption is due to the combined contributions from a strongly allowed $^1\pi\pi^*$ transition (L_a type) featured by the absorption band with a λ_{max} at ~280 nm and a weakly allowed $^1n\pi^*$ transition that constitutes to the tail of the absorption band and extends to ~340 nm.[5,6,8]

---

(8) (a) Ma, C. S.; Du, Y.; Kwok, W. M.; Phillips, D. L. *Chem.—Eur. J.* **2007**, *13*, 2290–2305. (b) Ma, C. S.; Kwok, W. M.; An, H. Y.; Guan, X. G.; Fu, M. Y.; Toy, P. H.; Phillips, D. L. *Chem.—Eur. J.* **2010**, *16*, 5102–5118.

The $^1\pi\pi^*$ transition is mainly responsible for the 267 nm photoabsorption, and it is straightforward that the observed initial strong ~330/360 nm transient fluorescence in the two solvents (see Figure 1) is from this excited state. The rather weak nature of the red-shifted (~400/420 nm) fluorescence seen at later times and especially the spectral blue shift of this fluorescence from ~420 nm in CH_3CN to ~400 nm in H_2O/CH_3CN solutions are diagnostic for its origination from a $^1n\pi^*$ character state. The relative blue shift of the electronic spectrum in a solvent capable of hydrogen-bonding (HB) interaction (such as the H_2O/CH_3CN solution used here) relative to that in a solvent that has little hydrogen-bonding ability (such as the neat CH_3CN solvent here) is a known effect characteristic of a $^1n\pi^*$ transition.[9] This effect arises from the presence in the former solvent of specific HB interactions between solvent molecule(s) and the lone pair electrons of the n orbital that causes energy destabilization of the $n \rightarrow \pi^*$ transition compared to that in the latter solvents that do not have this hydrogen-bonding effect. On the other hand, given the general small influence of the HB interaction on a $^1\pi\pi^*$ character transition, the substantial red shift of the $^1\pi\pi^*$ fluorescence in the H_2O/CH_3CN (~360 nm) solvent compared to that in the CH_3CN (~330 nm) solvent may reflect a solvent polarity induced energy stabilization of the $\pi \rightarrow \pi^*$ in the mixed aqueous solvent compared with in the neat CH_3CN solvent (the dielectric constants are ~78 and ~37 for H_2O and CH_3CN). This implies there is a sizable increase of the molecular dipole moment (i.e., a somewhat charge transfer (CT) character) in the $^1\pi\pi^*$ state in relation to the ground (S_0) state, which is well within expectation with regard to the electron-donating and -accepting properties of the methoxy and carbonyl groups, respectively, and the relative *para*-position of the two substituents, which is along the direction of the transition moment of the L_a type $\pi \rightarrow \pi^*$ electronic transition.

Using the above assignments, the rapid TRF decay and evolution can be taken as direct spectral manifestation for a prompt deactivation of the photoexcited $^1\pi\pi^*$ state by mainly an internal conversion (IC) to the $^1n\pi^*$ state ($\tau \approx$ 0.1 ps) and a subsequent decay of the $^1n\pi^*$ state in the two solvents ($\tau \approx 1$ or 1.3 ps, respectively). The analogous decay dynamics of the two states in the two solvents suggests that, though this process induces a wavelength shift of the correlated transient fluorescence spectra, the different properties (polarity and HB capability) of the two solvents have little influence on the deactivation behavior (e.g., the pathway and dynamics) of the two states. As confirmed by the TA results described below, the major deactivation channel responsible for the fast $^1n\pi^*$ depopulation is intersystem crossing (ISC) to a *p*MP chromophore localized triplet state. The rapid ISC is consistent with the close to unity triplet yield reported in the literature for many aromatic carbonyl compounds.[2f,4,5,10] However, It is noted that, probably due to the very short lifetimes, the fluorescence data of the $^1\pi\pi^*$ and $^1n\pi^*$ states given here to best of our knowledge represent one of the few available time-resolved spectral characterizations of singlet character excited states involved in the photodeprotection of the α-keto PRPGs.

Femtosecond Transient Absorption (fs-TA) Spectroscopy. Figure 3 shows a comparison of the fs-TA results obtained for MPEP in neat CH_3CN and H_2O/CH_3CN mixed solvents recorded at various time intervals ranging from 0 to 5000 ps after the 267 nm photoexcitation. The TA spectra recorded before and after a 10 ps time delay between the pump and probe pulses are presented separately to better display the spectral evolution at the respective time regimes. Parallel results acquired for MPPP in the two solvents as well as that in $CF_3CHOHCF_3$ are displayed in Figure 4. The TA spectra recorded for MPPP in CF_3CH_2OH are very similar to those observed in H_2O/CH_3CN, and these data are given in Figure 2S in the Supporting Information. Comparison of the spectra obtained within 10 ps time delays for the two compounds in the different solvents reveals a common feature of the spectral evolution from an initial weak ~325 nm absorption (0.1 ps spectrum) into a much stronger but structure-less absorption with a λ_{max} at ~410 nm (10 ps spectrum). This spectral change is accompanied by an isosbestic point at ~335 nm indicating the occurrence of a dynamic state-to-state conversion. Examination of the temporal growth of the ~410 nm absorption as seen in the insets in Figures 3 and 4 reveals that the kinetics of the spectral conversion can be described by a single exponential function with a ~2–3 ps time constant. The spectral profiles of the 10 ps TA closely resemble the triplet spectra reported for related *para*-substituted aromatic carbonyl compounds including the reference compound methoxyacetophenone (**2**) (see Figure 3S in the Supporting Information) and *p*HP compounds.[5b] The spectra can thus be attributed to the *p*MP localized triplet ($^3\pi\pi^*$) absorption of the two compounds in the various solvents. Such an assignment is corroborated further by the TR^3 results presented in the next section. From this and the general correlation between the kinetics of the TA spectral transformation and the TRF dynamics of the $^1n\pi^*$ decay, the observed TA evolution can be ascribed to arise from the ISC of the excited state population from the $^1n\pi^*$ singlet to the $^3\pi\pi^*$ triplet of the two systems in the different solvents. The subtle difference of the time constants in the TA ($\tau \approx 2-3$ ps) and TRF ($\tau \approx 1-1.3$ ps) may be related to the fact that the two spectral methods detect different electronic transitions (up to the upper excited state in the TA spectra and down to the S_0 in the TRF spectra), which might be affected slightly differently by the accompanying excited state relaxation processes such as intramolecular vibrational relaxation (IVR) and IC.

In contrast to the very similar spectral evolution displayed by the TA spectra before 10 ps, the triplet spectra of the two compounds after 10 ps shows clearly different features in both the spectral decay dynamics and the evolution of the spectral profiles in the different solvents. For MPEP and MPPP in H_2O/CH_3CN and MPPP in the fluorine substituted alcohols, the temporal changes of the initial triplet TA in the time interval of ~10–50 ps exhibit a sharpening and development of some structured features in the ~400–430 nm wavelength range of the TA profile (see the insets in Figures 3 and 4). This is not seen in the counterpart spectra of the two compounds in neat CH_3CN. This solvent dependence suggests that certain solvent effects are present only in the former type of hydrogen-bonding solvents and that these

---

[9] Turro, N. J. *Modern Molecular Photochemistry*; Benjamin/Cummings: Menlo Park, CA, 1978.

[10] (a) Ma, C. S.; Chan, W. S.; Kwok, W. M.; Zuo, P.; Phillips, D. L. *J. Phys. Chem. B* **2004**, *108*, 9264–9276. (b) Ma, C. S.; Zuo, P.; Kwok, W. M.; Chan, W. S.; Kan, J. T. W.; Toy, P. H.; Phillips, D. L. *J. Org. Chem.* **2004**, *69*, 6641–6657.

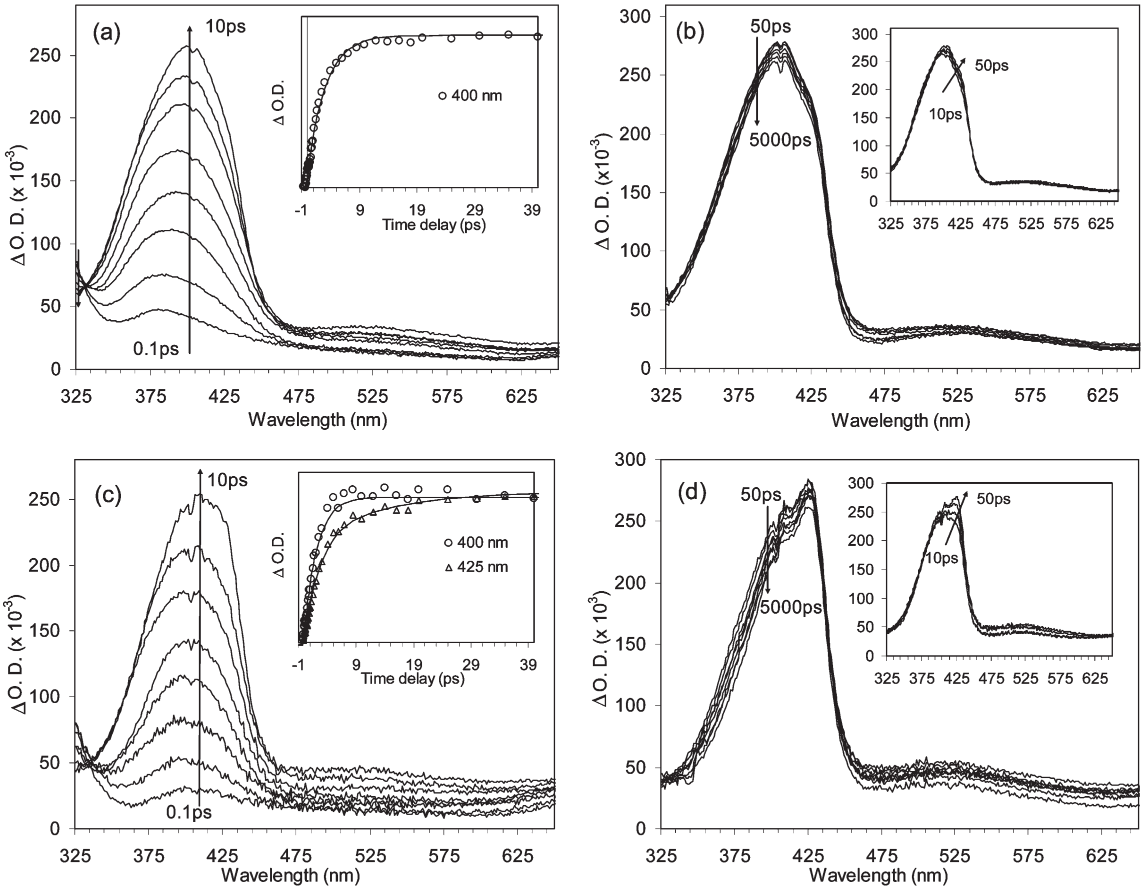

FIGURE 3. Fs-TA spectra of MPEP obtained with 267 nm excitation in (a, b) CH_3CN and (c, d) H_2O/CH_3CN. The insets in panels a and c show early time TA profiles at the indicated wavelengths; the solid lines are from IRF convolved exponential fitting of the experimental data. The insets in panels b and d display the temporal evolution of the TA spectra at a time range of ~10−50 ps. The arrows indicate the direction of the spectral evolution in the two solvents.

solvents can induce noticeable modification of the spectral character of the triplet absorption. Examination of the correlated TA time profiles at ~420 nm (see the insets in Figures 3 and 4) found a rise time of ~12 and ~20 ps for the growth dynamics of the structural profiles in H_2O/CH_3CN and the fluorinated alcohol solvents, respectively. To help resolve the nature of the solvent effects and the particular moiety of MPEP and MPPP that is responsible for the solute−solvent interaction, control experiments were done on the reference compound **2**, which has the same *p*MP chromophore but has no leaving group. As displayed in Figure 3S in Supporting Information, the TA spectra acquired for **2** in neat CH_3CN and H_2O/CH_3CN mixed solvent are very similar and also closely resemble the spectra recorded for MPEP and MPPP in neat CH_3CN. The lack of the ~400−430 nm structured feature for **2** even in H_2O/CH_3CN is in contrast to the appearance of this feature observed for MPEP and MPPP in the same solvent. This observation of the leaving group dependence suggests a relevance of the leaving group to the solvent effect that affects the triplet absorption. These results suggest that the temporal development of the ~400−430 nm feature showed exclusively by the triplet of MPEP and MPPP in the water-containing and fluorinated alcohol solvents may originate from a dynamic process associated with the partial solvation of the respective leaving groups of the two compounds by the surrounding solvent molecules. This is consistent with the known ability of water and fluorinated alcohols in promoting solvation of an anionic group.[5b,11]

Apart from the different spectral character, the later time triplet absorption of MPEP and MPPP shows distinctly different decay dynamics in the different solvents. The triplet kinetics of MPEP (Figure 3) in neat CH_3CN and H_2O/CH_3CN are similar and show little decay within the several ns time window covered by the fs-TA measurements; unlike this, the MPPP triplet (Figure 4) exhibits increasingly faster decay as the solvent changes from CH_3CN to H_2O/CH_3CN or CF_3CH_2OH and to $CF_3CHOHCF_3$. A comparison of the TA decay traces of the MPPP triplet in these solvents is displayed in Figure 5. Exponential fitting of the data points resulted in time constants of ≫~20 ns, ~5.4 ns, and ~3.1 ns for the decay dynamics in CH_3CN, H_2O/CH_3CN or CF_3CH_2OH, and $CF_3CHOHCF_3$ solvents, respectively. The much faster triplet decay of MPPP upon changing the solvent from neat CH_3CN to the H_2O/CH_3CN mixed solvent (or CF_3CH_2OH) and to $CF_3CHOHCF_3$ indicates there is a significant involvement of an additional triplet deactivation channel in the latter solvents as compared to CH_3CN. Considering that the protic solvents are highly capable of encouraging heterolytic cleavage of a leaving group bearing a C−O bond and that the diphenyl phosphate in MPPP is a more

---

(11) Reichardt, C. *Solvent and Solvent Effect in Organic Chemistry*; VCH Verlag: Weinheim, 1988.

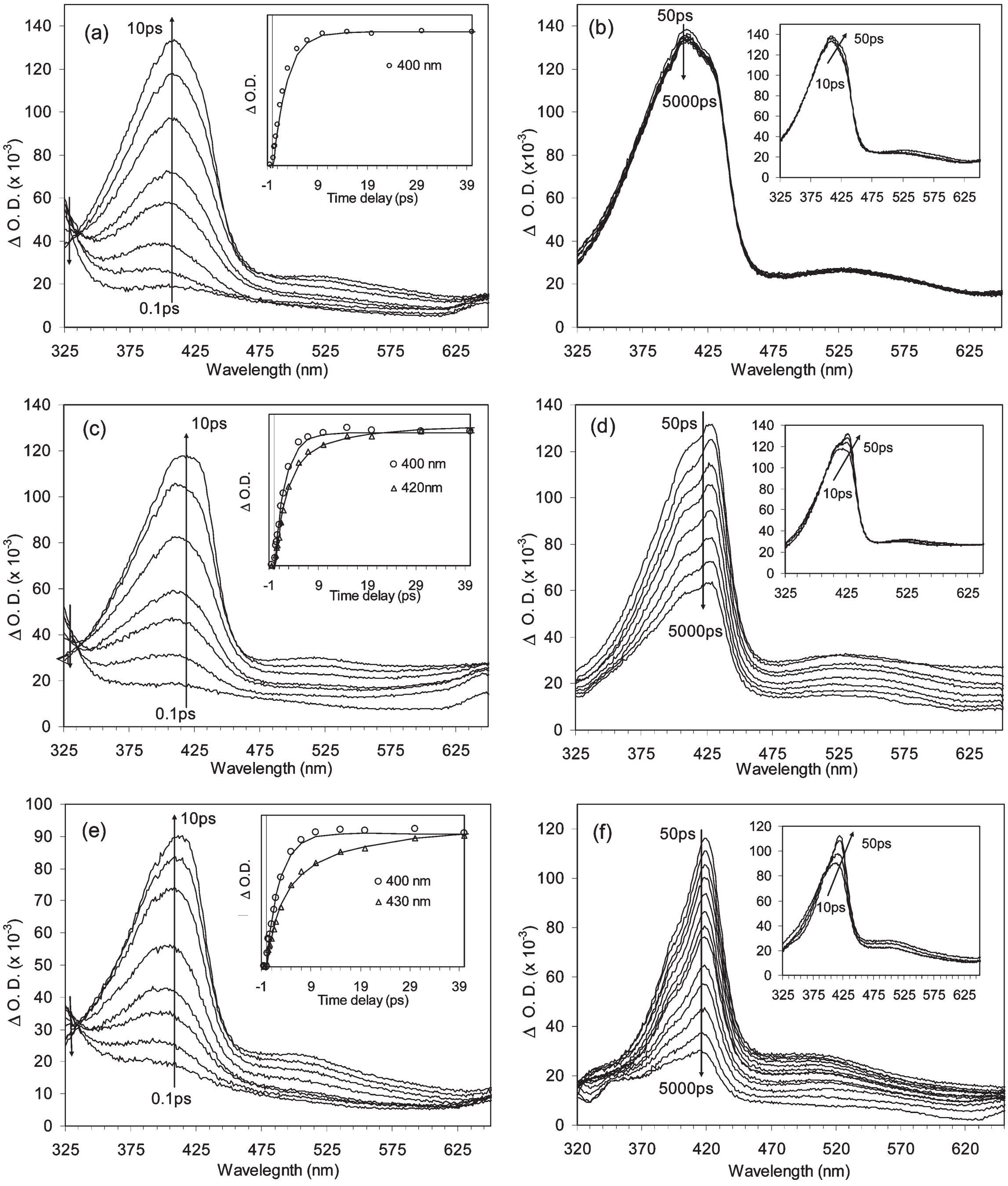

FIGURE 4. Fs-TA spectra of MPPP obtained with 267 nm excitation in (a, b) CH_3CN, (c, d) H_2O/CH_3CN, and (e, f) $CF_3CH(OH)CF_3$. The insets in panels a, c, and e show early time TA profiles at the indicated wavelengths; the solid lines are from IRF convolved exponential fitting of the experimental data. The insets in panels b, d, and f display the temporal evolution of the TA spectra over a time range of ~10−50 ps. The arrows indicate the spectral evolution in different solvents.

labile leaving group than the diethyl phosphate in MPEP,[5b,11] this observation may imply the occurrence within a several nanosecond scale of a competitive solvent assisted heterolytic liberation of the leaving group from the triplet of MPPP in these solvents. To further explore this and to get some insight into the structural nature and reactivity of the relatively long-lived triplet of MPEP in the various solvents and MPPP in CH_3CN, TR^3 measurements have been designed and preformed for the two systems in both the picosecond and nanosecond time regimes.

Picosecond and Nanosecond Time-Resolved Resonance Raman Spectroscopy. The ps-TR^3 measurements with 267 nm/400 nm pump/probe wavelengths and ns-TR^3 acquired with 266 nm/416 nm pump/probe wavelengths for MPEP and MPPP were done in the various solvents. With reference to the TA spectra obtained for the two compounds (Figures 3 and 4), the 400 and 416 nm probe wavelengths were chosen to detect selectively the resonance Raman spectra of the triplet state for the two systems in the different solvents. Figure 6 shows the representative ps-TR^3 and ns-TR^3 spectra of MPEP recorded in neat CH_3CN and mixed H_2O/CH_3CN solvent. The counterpart ns-TR^3 results obtained for MPPP in the two solvents are displayed in Figure 7. Ns-TR^3 spectra obtained for MPEP and MPPP in CF_3CH_2OH are very similar to the corresponding data acquired in the water-mixed solvents and are given in Figure 4S in the Supporting Information. It can be seen from Figure 6 that the same vibrational features were observed for MPEP in the two solvents both in the late ps-TR^3 spectra and the corresponding ns-TR^3 spectra. Comparison of the MPPP ns-TR^3 spectra with the counterpart MPEP data reveals observation of analogous Raman features which indicates a very similar structural character for the two compounds in the respective solvents. It is noted that the general TR^3 feature in the resonance enhancement profile and vibrational frequencies observed for the triplet spectra of MPEP and MPPP in neat CH_3CN and the water-mixed solvent resemble those reported for the triplet spectra of the reference compound **2** and *p*HP caged compounds in the corresponding solvents. This corroborates the assignment of the TR^3 spectra to the triplets of MPEP and MPPP and suggests further that the vibrational features revealed in the spectra originate mainly from the common *p*MP chromophore of the two compounds.

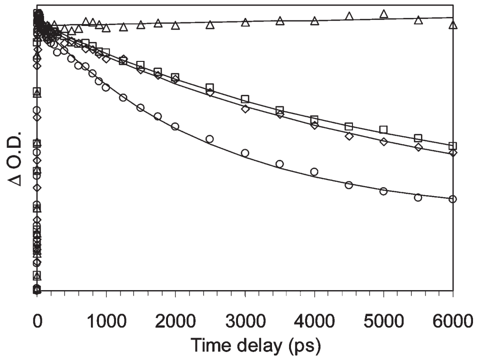

FIGURE 5. Normalized TA decay profiles of MPPP at the 400 nm wavelengths observed with the 267 nm excitation in (△) CH_3CN, (◇) H_2O/CH_3CN, (□) CH_3CH_2OH, and (○) $CF_3CH(OH)CF_3$. The solid lines show the instrumental response function (IRF) convolved exponential fittings to the experimental data.

Close examination of the TR^3 spectra and spectral evolution obtained for MPEP and MPPP (Figures 6 and 7) reveals several important observations in terms of the significant solvent and leaving group dependent triplet decay dynamics and some distinct solvent dependent vibrational features of the triplet spectra for MPEP and MPPP in the solvents studied. Regarding the triplet decay, Figure 8 displays the decay kinetics obtained by fitting the Raman features with Lorentzian band shapes for the two compounds in neat CH_3CN and a H_2O/CH_3CN mixed solvent. The kinetics can be fit reasonable well by single exponential function with time constants estimated to be ~80 and ~130 ns for MPEP in CH_3CN and H_2O/CH_3CN solvents,

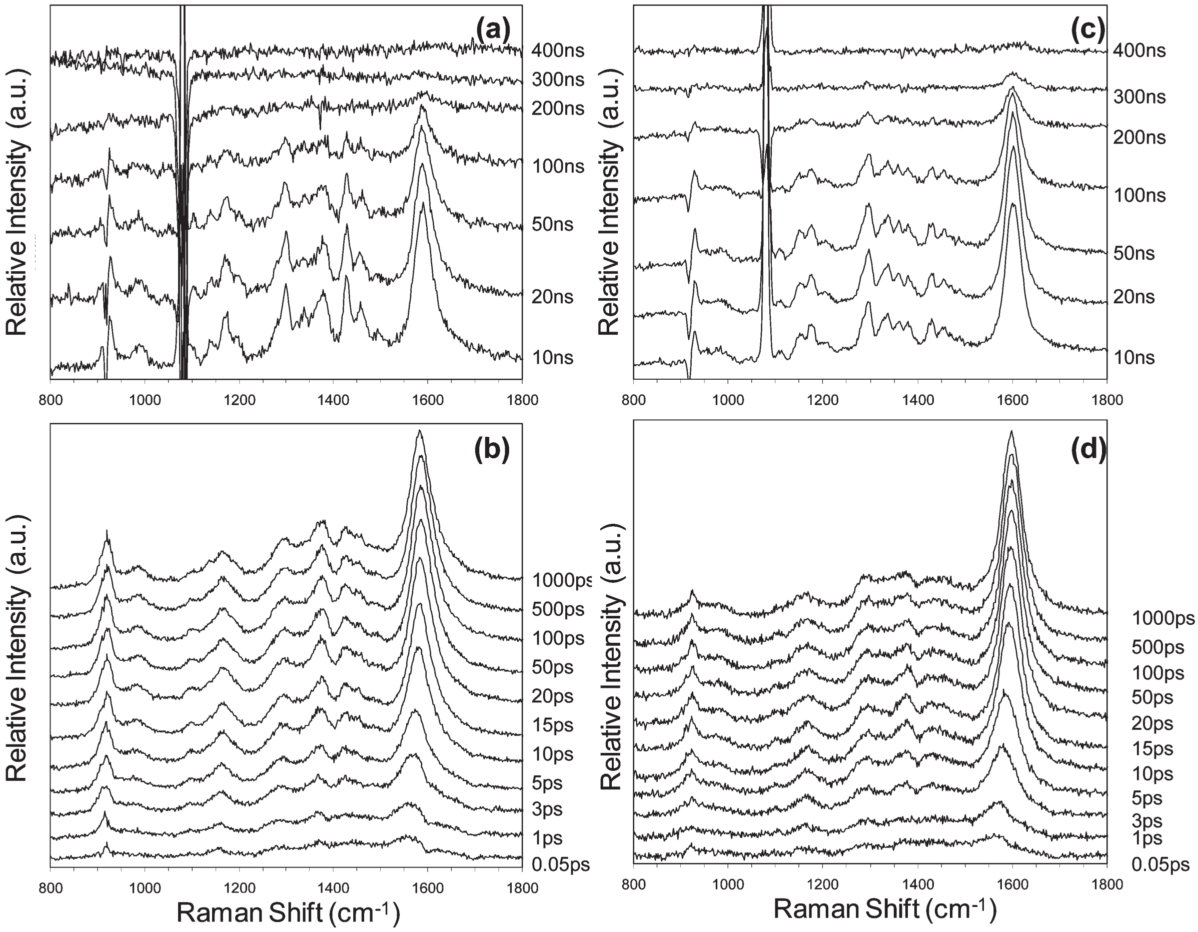

FIGURE 6. Shown are ns-TR^3 (a, c) and ps-TR^3 (b, d) spectra of MPEP in neat CH_3CN (a, b) and H_2O/CH_3CN (1:1, v/v) (c, d) obtained with a 266 nm pump excitation wavelength and 400 nm (ps-TR^3) and 416 nm (ns-TR^3) probe wavelengths at various delay times that are indicated next to the spectra.

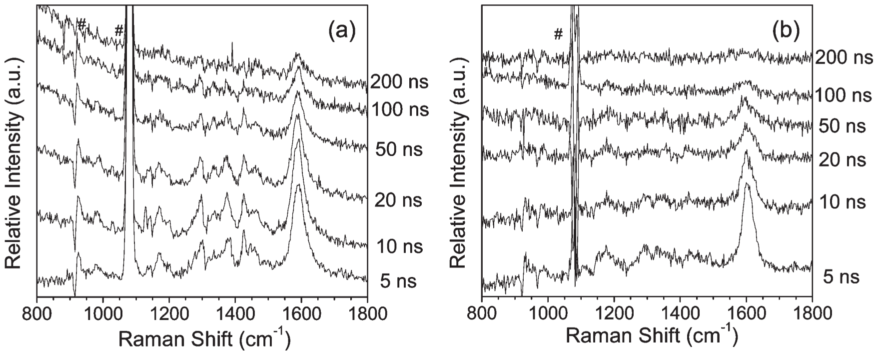

FIGURE 7. Ns-TR^3 spectra of MPPP in (a) neat CH_3CN and (b) a H_2O/CH_3CN (1:1, v/v) mixed solvent obtained with a 266 nm pump excitation wavelength and a 416 nm probe wavelength at various delay times that are indicated next to the spectra are displayed. The # is due to a stray laser line.

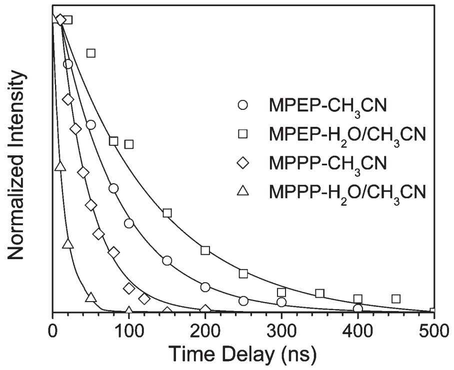

FIGURE 8. Time dependences of the MPEP (*o*) and MPPP (◇) triplet ~1590 cm^{-1} band in CH_3CN and the MPEP (□) and MPPP (Δ) triplet ~1604 cm^{-1} band in H_2O/CH_3CN (1:1, v/v) mixed solvent obtained in ns-TR^3 spectra of MPEP and MPPP displayed in Figures 6 and 7, respectively. The solid lines are results of one exponential fitting of the experimental data points.

respectively and ~40 and ~10 ns for MPPP in the same two solvents, respectively. The kinetics data and time constants derived for the two compounds in CF_3CH_2OH were found to be very close to the corresponding results obtained in the water-mixed solvent, and these data are given in Figure 5S in the Supporting Information. It is remarkable from Figure 8 that the decay time of the triplet shows a substantial increase for MPEP in neat CH_3CN as compared to that in the water-mixed solvent or the CF_3CH_2OH solvent. This is in stark contrast to the marked decrease in the triplet lifetime observed for MPPP upon changing from the former to latter solvents. The very fast triplet decay observed for MPPP in H_2O/CH_3CN and CF_3CH_2OH coincides with the rapid quenching of the triplet absorption revealed by the fs-TA measurements for the same compound in the corresponding solvents. Considering the ~10 ns time resolution of the present ns-TR^3 experiments, it is reasonable that, for the measurements of triplet decay dynamics for MPPP, the ~10 ns decay time constant estimated on the basis of the ns-TR^3 spectra can be considered as an upper limit and the ~5.4 ns decay time constant provided by the fs-TA data may serve more reliably in these solvents.

The observation that the triplet of MPEP shows a slower decay in the protic than aprotic solvent appears to be rather unexpected but is reminiscent of the solvent effect reported earlier in a TR^3 study of the reference compound **2** in various solvents including the neat CH_3CN and mixed H_2O/CH_3CN solvents.[12] That study observed a much prolonged triplet lifetime accompanied by some noticeable changes in the intensity distribution pattern and vibrational frequencies of some Raman bands in the triplet TR^3 spectra of **2** in the H_2O/CH_3CN solvent (~160 ns lifetime) as compared to that in the neat CH_3CN solvent (~40 ns lifetime).[12] Density functional theory (DFT) calculations that took into consideration the specific solvent−solute H-bonding interaction of one or two water molecules with the compound **2** revealed that this solvent effect is associated with the well-known increase of the basicity of the carbonyl group upon triplet formation and is caused mainly by the development in the triplet (relative to the S_0 state) of a strengthened H-bonding interaction between the carbonyl oxygen and the surrounding solvent molecule(s) that could be present only in the protic solvent.[5,12,13] The H-bonding was observed to induce a profound modification of the electronic and geometric structures of the triplet making the H-bonded triplet to have a more phenyl ring localized $\pi\pi^*$ character with an enhanced ring quinoidal feature and a tendency to have a longer lifetime than that of the "free" triplet of the quantum mechanical mixed $n\pi^*/\pi\pi^*$ character in the aprotic solvent.[10,12−14] To further examine the situation for the triplet of MPEP, a careful comparison has been made between the ns-TR^3 (or > 50 ps late time ps-TR^3) spectra of MPEP in CH_3CN with those in the H_2O/CH_3CN or CF_3CH_2OH solvents and this comparison is shown in Figure 9. Inspection of the spectra in Figure 9 shows some clear differences between the spectra in the two types of solvents; several features show frequency shifts and there are obvious divergences in the relative intensities of the Raman bands especially in the 1350−1500 cm^{-1} spectral region. These spectral variations are analogous to that reported for **2** and imply that the carbonyl H-bonding effect may also apply to the MPEP triplet and contribute to the spectral and lifetime differences observed in the different solvents here. In particular, the frequency upshift (by ~15 cm^{-1}) displayed by the ring central

---

(12) Chan, W. S.; Ma, C. S.; Kwok, W. M.; Phillips, D. L. *J. Phys. Chem. A* **2005**, *109*, 3454–3469.

(13) (a) Zuo, P.; Ma, C. S.; Kwok, W. M.; Chan, W. S.; Phillips, D. L. *J. Org. Chem.* **2005**, *70*, 8661–8675. (b) Rauh, R. D.; Leermakers, P. A. *J. Am. Chem. Soc.* **1968**, *90*, 2246–2249. (c) Nakayama, T.; Otani, A.; Hamanoue, K. *J. Chem. Soc., Faraday Trans.* **1995**, *91*, 855–861. (d) Ramseier, M.; Senn, P.; Wirz, J. *J. Phys. Chem. A* **2003**, *107*, 3305–3315.

(14) (a) Fang, W. H.; Phillips, D. L. *ChemPhysChem* **2002**, *3*, 889–892. (b) Chen, X. B.; Ma, C. S.; Kwok, W. M.; Guan, X. G.; Du, Y.; Phillips, D. L. *J. Phys. Chem. A* **2006**, *110*, 12406–12413.

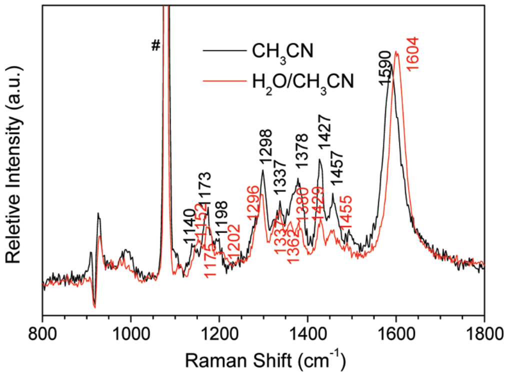

FIGURE 9. Comparison of the ns-TR^3 of MPEP obtained in CH$_3$CN and H$_2$O/CH$_3$CN (1:1, v/v) mixed solvent with a 266 nm pump excitation wavelength and a 416 nm probe excitation wavelength at a time delay of 10 ns.

C=C stretching vibration of the MPEP triplet on going from CH$_3$CN (1590 cm^{-1}) to the mixed H$_2$O solvent (1604 cm^{-1}) is consistent with this. This is one of the characteristic indications for the enhanced quinoidal ring feature of the triplet in the latter protic solvent compared to the former nonprotic solvent. It is noted that a similar variation in the spectral appearance is also observed for MPPP in these two solvents as well (see the 5 ns TR^3 spectra in Figure 7a and b), implying there is also the involvement of the carbonyl H-bonding irrespective of the constituent of the leaving group.

It is interesting to note that the spectral differences shown by MPEP and MPPP in the protic versus aprotic solvents appear to be not as much as that reported for **2** in the corresponding solvents. An example of this is that the corresponding frequency upshift of the ring C=C stretching was observed to be ~30 cm^{-1} in the triplet of **2**, which is nearly double the amount seen here for the triplet of MPEP and MPPP. This difference may be associated with the additional presence of the leaving group in MPEP and MPPP in comparison to **2**, which could influence the charge density of the carbonyl oxygen and affect the strength of the H-bonding interaction. Provided that the strength of the carbonyl H-bonding correlates with the degree of the $\pi\pi^*$ electronic component of the triplet state, the lesser extent of H-bonding may imply that MPEP and MPPP, like most of the related aromatic carbonyls,[10,14] have triplet states of largely mixed nπ^*/$\pi\pi^*$ character with a modestly increased $\pi\pi^*$ character relative to the nπ^* contribution in the protic solvent compared to the aprotic solvent. This intrinsic electronic feature of the triplet has important implications in understanding the solvent dependent reductive versus rearrangement deprotection reactivity of the two compounds reported in the literature.[2b,c,6a,b]

The TR^3 spectra recorded at early picoseconds time delay (Figure 6b and d, < 50 ps) exhibit substantial temporal changes that characterize directly the dynamical evolution from the initial (< 3 ps) to the final (the later time) triplet spectrum of MPEP in neat CH$_3$CN and mixed H$_2$O/CH$_3$CN solvents. Comparison of the spectra shows a rapid growth of the triplet spectrum accompanied by a gradual frequency upshift and bandwidth narrowing of some Raman features within ~50 ps after the photoexcitation. For instance, on going from 3 to 50 ps, the feature associated with the ring C=C stretching exhibits a frequency shift from ~1565 to ~1585 cm^{-1} in CH$_3$CN and from 1580 to 1600 cm^{-1} in H$_2$O/CH$_3$CN along with a ~20 cm^{-1} narrowing of the bandwidth in both of the solvents. This observation of a simultaneous frequency and bandwidth variation of the vibrational bands on the tens of ps time scale is typical for energy relaxation processes of the related excited-state species.[10,15] The TR^3 intensity and spectral evolution observed here can thus be ascribed to the convolved processes of ISC ($\tau \approx 2-3$ ps) with some energy and/or conformation relaxation in the different solvents. Considering the massive excess energy that the 267 nm photoexcitation could introduce into the nascent triplet state (a typical triplet state has an energy of 69−71 kcal/mol), it is quite certain that there is some dynamical relaxation of the excess vibrational energy in the triplet manifold contributing to the processes observed in the ps spectra. For the cases taking place in the water-mixed solvent and also in the fluorinated alcohol solvents, in addition to the excess energy relaxation, solvation related relaxation such as dynamical reorientation of solvent molecules in response to the solvation of the leaving group and the development of the carbonyl located H-bonding could also be involved and account jointly for the observed early time TR^3 temporal evolution. Taken together with the observed solvent specific spectral features revealed in the later time TR^3 spectra, it is noticeable that, among the various vibrational bands seen in the TR^3 spectra, the ~1590−1605 cm^{-1} band of the ring central C=C stretching mode appears to be distinctive in terms of being representative of a particular solvation configuration and the consequently induced subtle modification of the *p*MP triplet structure in the protic versus aprotic environments.

Combining the fs-TA and ps/ns-TR^3 results for the triplet states of MPEP and MPPP indicates that these triplet states have nπ^*/$\pi\pi^*$ mixed character and are present in the solvent associated form with the decay dynamics governed by the lability of the leaving group and the properties of solvent. The tens to hundred ns decay dynamics observed for the two compounds in neat CH$_3$CN solvent and MPEP in the other tested solvents occur on a similar time scale as that reported for the reference compound **2**[12] and *p*HP compounds in the inert CH$_3$CN solvent.[5,10,13a] It can be inferred from this that the major deactivation event(s) underlying the triplet decay for these systems would be the diffusion controlled oxygen quenching of the triplet[9] and other possible decay channel(s), such as the deprotection *via* either the reductive or rearrangement reactions, if involved, could occur only to a very limited extent. The much faster triplet decay ($\tau \approx 5.4$ ns) of MPPP in the H$_2$O/CH$_3$CN and fluorinated alcohols compared to that in neat CH$_3$CN (Figures 5 and 8) is analogous to that reported for the *p*HP phosphates (HPPP and HPEP, eq 2) in the corresponding solvents.[5,16] The latter is caused by heterolytic liberation of the leaving group followed by a stepwise solvolytic rearrangement with the time constant of the

---

(15) (a) Liard, D. J.; Busby, M.; Matousek, P.; Towrie, M.; Vlcek, A. *J. Phys. Chem. A* **2004**, *108*, 2363–2369. (b) Liard, D. J.; Busby, M.; Farrell, I. R.; Matousek, P.; Towrie, M.; Vlcek, A. *J. Phys. Chem. A* **2004**, *108*, 556–567. (c) Hester, R. E.; Matousek, P.; Moore, J. N.; Parker, A. W.; Toner, W. T.; Towrie, M. *Chem. Phys. Lett.* **1993**, *208*, 471–478. (d) Matousek, P.; Parker, A. W.; Towrie, M.; Toner, W. T. *J. Chem. Phys.* **1997**, *107*, 9807–9817. (e) Ma, C.; Kwok, W. M.; Matousek, P.; Parker, A. W.; Phillips, D.; Toner, W. T.; Towrie, M. *J. Raman Spectrosc.* **2001**, *32*, 115–123. (f) Weaver, W. L.; Huston, L. A.; Iwata, K.; Gustafson, T. L. *J. Phys. Chem.* **1992**, *96*, 8956–8961. (g) Iwata, K.; Hamaguchi, H. *J. Phys. Chem. A* **1997**, *101*, 632–637.

(16) Cao, Q.; Guan, X. G.; George, M. W.; Phillips, D. L.; Ma, C. S.; Kwok, W. M.; Li, M. D.; Du, Y.; Sun, X. Z.; Xue, J. D. *Faraday Discuss.* **2010**, *145*, 171–183.

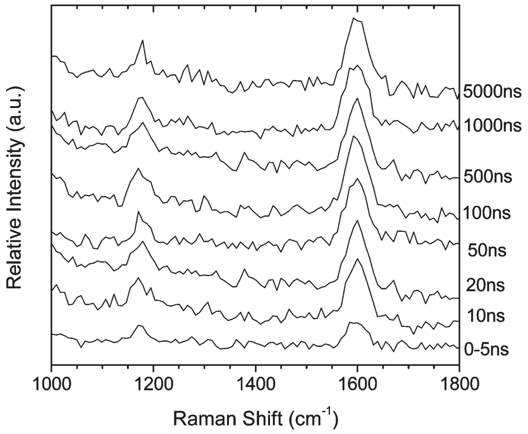

FIGURE 10. ns-TR^3 spectra of MPPP in a H_2O/CH_3CN (1:1, v/v) mixed solvent obtained with a 266 nm pump excitation wavelength and a 223 nm probe wavelength at various delay times that are indicated next to the spectra.

triplet cleavage taking place on the hundreds of ps time scale in the water/CH_3CN mixed solvents. To explore the particular reaction that is responsible for the rapid triplet quenching of MPPP in these solvents and also to make a connection with and to determine the rate of the *p*MP rearrangement deprotection reaction, photochemistry experiments and ns-TR^3 measurements were done to directly detect the formation dynamics of the rearrangement product for MPPP in the water/CH_3CN mixed solvent and the CF_3CH_2OH solvent.

Photochemistry and Nanosecond Time-Resolved Resonance Raman Spectroscopy Experiments To Probe the Rearrangement Product Formation for MPPP in a Water/CH_3CN Mixed Solvent and a CF_3CH_2OH Solvent. Consistent with the major photoproduct reported for MPPP in the literature,[1a,2] the UV−vis spectra and spectral transformation (Figure 1S in the Supporting Information) observed in the photochemistry experiments for the photolysis of MPPP in the H_2O/CH_3CN (1:1, v/v) mixed solvent or in the CF_3CH_2OH solvent indicate the photodeprotection and rearrangement reactions leading to release of the phosphate leaving group and formation of the solvolytic rearrangement products takes place under these conditions. Referring to the clearly different absorption profiles exhibited by the MPPP and the MPAA (**3**) product (spectrum at 0 and 60 s in Figure 1S in the Supporting Information), a 223 nm probe wavelength was chosen in the ns-TR^3 measurements to selectively follow the dynamics of the formation of MPAA after the 267 nm photoexcitation of MPPP in the two different solvents. The spectra obtained in the H_2O/CH_3CN mixed solvent are displayed in Figure 10. A very similar result is observed in a CF_3CH_2OH solvent, and this data is given in Figure 6S in the Supporting Information.

The ns-TR^3 spectra (Figure 10) reveal that there are two main Raman bands at ~1178 and ~1600 cm^{-1} that can promptly be observed after excitation and appear to be stable up to the tens of microseconds time scale after the photoexcitation. These spectral features and the overall TR^3 spectral profile are nearly identical to the resonance Raman spectrum reported for an authentic sample of HPAA obtained with the same probe wavelength and under the same solvent conditions.[5b] This result provides explicit experimental evidence for the formation of a similar rearrangement product MPAA from the photolysis of MPPP in a water-mixed solvent. Obviously, a similar perspective applies to the reaction taking place in the CF_3CH_2OH solvent. Examination of the time-dependence of the MPAA TR^3 spectra (Figure 11, Figure 7S in the Supporting Information) shows a time resolution limited time constant of ~10 ns for the growth of the product in the two different solvents. This product formation dynamics appears to correlate well with the triplet decay dynamics ($\tau \approx 5.4$ ns) observed in the fs-TA (Figures 4 and 5) and ns-TR^3 (Figures 7 and 8) in the corresponding solvents. This is consistent with a concerted triplet deprotection and solvolytic rearrangement mechanism for MPPP in the two solvents, though given the uncertainty associated with the ~10 ns time resolution of the ns-TR^3 measurements, it might also be possible that there is a stepwise pathway of the triplet deprotection followed by a rapid, nearly concurrent rearrangement reaction.

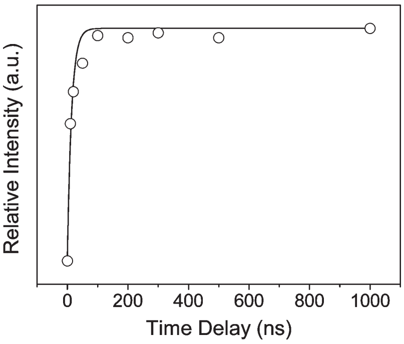

FIGURE 11. Time dependence of the ~1600 cm^{-1} band in H_2O/CH_3CN (1:1, v/v) mixed solvent obtained in the ns-TR^3 spectra displayed in Figure 10. The solid line is from a one exponential fitting of the experimental data points.

On the basis of all of the experimental results presented, it can be concluded that the following photochemical reactions are induced by the 267 nm excited MPEP and MPPP in the various solvents (Scheme 1)

This deprotection reactivity of the *p*MP triplet differs clearly from that established for the *p*HP triplet.[5b] The heterolytic liberation of the leaving group was observed to take place very rapidly ($\tau \approx 150$ ps) for the triplet of HPPP in the mixed H_2O/CH_3CN (1:1, v/v) solvent. This is much faster (and therefore more efficient) than the deprotection of MPPP in the same solvent. In contrast to the minor reactivity of MPEP, the deprotection of HPEP is very efficient and takes place with $\tau \approx 420$ ps in the water-containing solvent. The obviously different reactivity of the *p*MP to *p*HP triplets suggests that a crucial effect is associated with replacing the hydroxy group by the methoxy group. To provide molecular insight into this, reaction pathway calculations using the DFT ((U)B3LYP/6-31G*) method that take into consideration of the specific solvent effect of the water molecules have been done to investigate the structures, transition states, and driving force for the *p*MP triplet deprotection in a water-containing solvent.

Density Function Theory (DFT) Calculation for the MPPP Triplet Deprotection. With reference to our previous calculations for the triplet deprotection of HPEP and HPA (eq 2),[14,16,17] a simple model with the involvement of four water molecules was adopted for the comparative DFT calculations performed for MPPP and HPPP. To mimic the relevant features of the solvent associated configuration

---

[17] Chen, X. B.; Ma, C. S.; Kwok, W. M.; Guan, X. G.; Du, Y.; Phillips, D. L. *J. Phys. Chem. B* **2007**, *111*, 11832–11842.

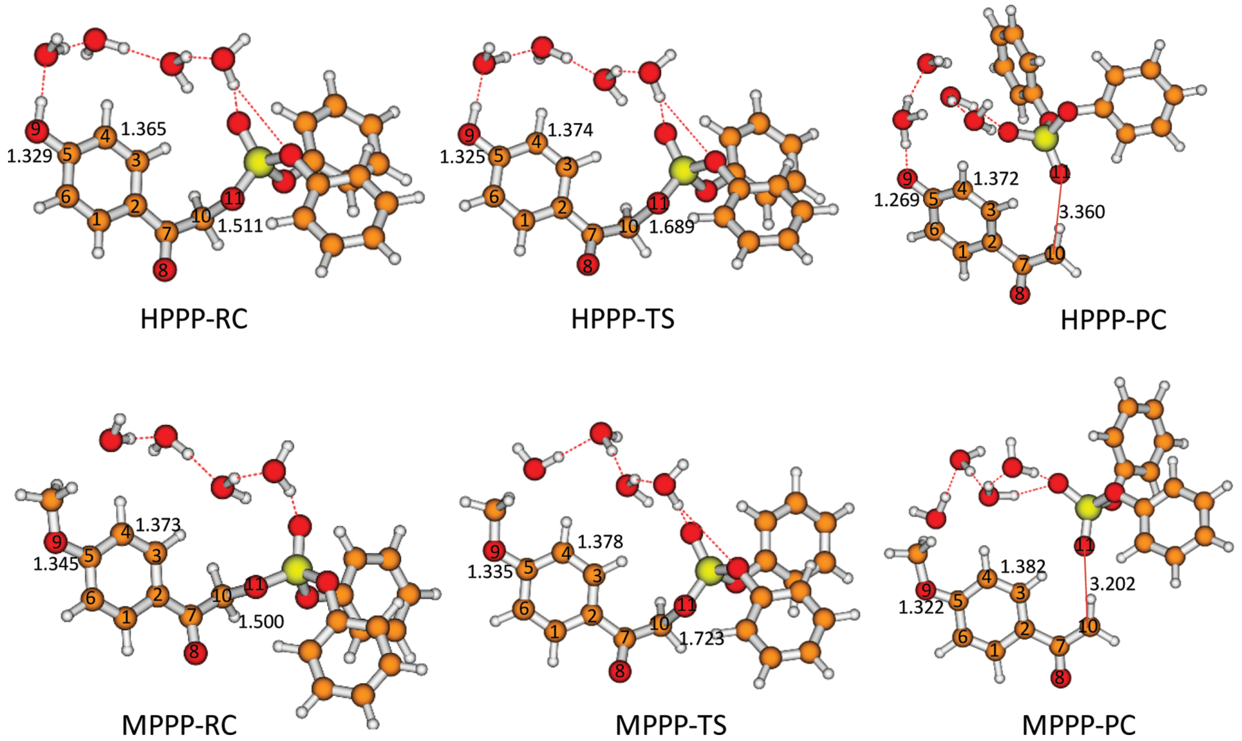

FIGURE 12. Optimized geometries obtained from (U)B3LYP/6-31G* computations for the reaction complexes (RC), transition states (TS), and product complexes (PC) of the triplet deprotection reactions of HPPP and MPPP with four water molecules explicitly solvating the system.

SCHEME 1

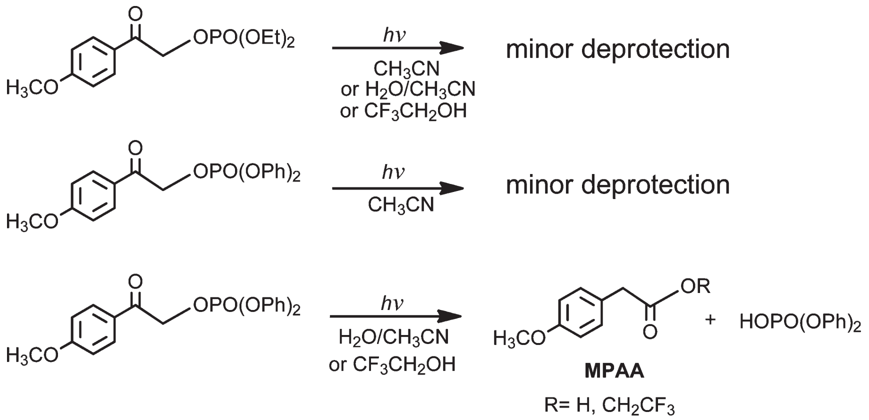

revealed in the fs-TA and ns-TR^3 results, the water molecules were arranged in a spatial range that allows interaction with the diphenyl phosphate leaving group on one side and the hydroxyl (HPPP) or methoxy (MPPP) group on the other side (see Table 2S in the Supporting Information for the detailed Cartesian coordinates and total energies of the complexes involved in the reactions). This simple model for the solvation of the molecule is not meant to imply there is a well-defined four water solute system but rather allows the water solvent molecules to simultaneously interact with the leaving group on one side and the hydroxyl or methoxy group on the other side while allowing a partial hydrogen bonding network between the water molecules interacting with the two sides of the solute molecule. This is crudely similar to having the solute molecule enmeshed in a hydrogen-bonded water network that can interact strongly simultaneously with the leaving group on one side and the hydroxyl or methoxy group on the other side while having a hydrogen bond water network surrounding the solute. This crude four water-solute model was computationally tractable for our limited computer resources and allowed an exploration of the one-side (MPPP) versus two-side (HPPP) solvation effects so as to better understand the different activity for the reactions of interest. More sophisticated calculations using many more water molecules along with a QMMM approach would better mimic the actual solvent−solute interactions and may provide even deeper insight in the future into the differing reactivity observed for the systems examined here with a simpler approach. Figure 12 shows the optimized structures found for the triplet reaction complexes (RC), the transition states (TS), and product complex (PC) for the MPPP and HPPP reactions. The barrier crossing in both of the systems leads to a heterolytic cleavage of the C10−O11 bond to yield a contact ion

TABLE 1. Key Geometry Information of HPPP and MPPP Reactant Complexes (RC) and Transition States (TS)[a]

	HPPP-4w complex			MPPP-4w complex		
	RC	TS	diff	RC	TS	diff
bond length of C10−O11 (Å)	1.511	1.689	0.178	1.500	1.723	0.223
Mulliken charge of C10	−0.149	−0.198	−0.049	−0.142	−0.206	−0.064
Mulliken charge of O11	−0.519	−0.543	−0.024	−0.520	−0.549	−0.029
$\Delta G^{\ddagger}$(kcal/mol)		1.14			3.04	

[a] Obtained at the (U)B3LYP/6-31G* level of theory for the C and O atoms where the cleavage occurs in the deprotection reactions.

pair character PC which is composed of the water-solvated phosphate anion and the counterpart cation of the *p*MP or solvated *p*HP moiety. It is clear from Figure 12 that, in both the RC and TS, the four water molecules involved in the reaction form a water chain via H-bonding, by interacting through the H-bonding of the two ends of the molecule (e.g., with the leaving group and the phenolic hydrogen, respectively). This chain of water molecules forms and works as a water bridge in the case of HPPP (denoted hereafter as two-sided solvation); such a bridge is however not observed for MPPP because the change of the hydroxy moiety by the methoxy moiety makes it unlikely to have an analogous interaction at the methoxy site and thus leaves available only the solvation at the leaving group side of the molecule (denoted hereafter as one-sided solvation). A direct consequence of the different solvation configurations in HPPP versus MPPP is the larger extent of the electronic conjugation between the ring and the electron-donating oxygen in the former case than in the latter system. This is manifested by the shorter bond lengths observed in the RC for the related bonds of the C5−O9 and ring center C=C in HPPP (∼1.365 Å for C4−C3/C1-C6) than found in MPPP (∼1.375 Å for C4−C3/C1−C6). This is in agreement with the vibrational frequency results observed for the corresponding modes in the TR^3 spectra, for example, the C=C stretching is at higher frequency in HPPP (∼1620 cm^{-1})[5b] than MPPP (∼1605 cm^{-1}, Figure 7b) reflecting more tightening of the bond in HPPP than in MPPP.

The calculated free energy barriers are ∼1.14 kcal/mol for HPPP and ∼3.04 kcal/mol for MPPP. These low activation energies are consistent with the generally rapid triplet reactions observed experimentally for HPPP (∼150 ps) and MPPP (∼5.4 ns) in the water/CH_3CN mixed solutions. The substantial higher deprotection barrier in MPPP than in HPPP is in agreement with the experimentally observed slower triplet decay of MPPP compared to HPPP. Comparison of the calculated results on the relevant structures and charge distributions of the RCs and TSs for MPPP and HPPP contains further useful information about the origin of the different barrier heights exhibited by the two systems. Table 1 lists the representative data of the calculated bond lengths and associated charge densities for the related C−O bond cleavage deprotection reactions. It can be seen from the table that the two systems generally display modest changes in the structure and charge distribution upon going from their respective RC to TS. This suggests there is an early transition state feature for the barrier leading to deprotection in MPPP and HPPP. A closer comparison observes a higher degree of similarity between the relevant RC to TS in HPPP than in MPPP. This means there is an easier access to the TS in HPPP than in MPPP. This corroborates the lower barrier found for HPPP than MPPP and implies further that the structure of the RC plays a key role in determining the accessibility of the activation barrier and the dynamics of the deprotection reaction. Within the context of this and the fact that the RC structure is affected sensitively by the solvation configuration (Figure 12), it is reasonable that the less favorable one-side solvation configuration in MPPP relative to the two-side solvation in HPPP may constitute an important factor to account for the reduced reactivity of the MPPP triplet compared to the HPPP triplet.

The above results underscore the necessity of the specific solvation interaction in driving and assisting the triplet cleavage reactions. Indeed, our previous calculations on the HPEP triplet deprotection reaction found that, compared to the case without the explicit involvement of the hydrogen-bonded water molecules, the incorporation of the four water molecules leads the free energy barrier to drop substantially.[16] Analogous calculations for MPEP and MPPP observed a similar trend (see Table 1S in the Supporting Information). The strong increase in the activation barrier height brought about by the absence of the water molecules explains the experimentally observed negligible triplet reactivity of these compounds in neat CH_3CN.

Additionally, in line with the experimental results, our preliminary comparative calculations have also observed a trend of a much lower barrier for the MPPP than MPEP triplet reactions. This provides theoretical evidence to indicate that a more labile leaving group favors the triplet cleavage, or in other words, solvation of the leaving group plays an important role in promoting the triplet liberation of the leaving group. The leaving group solvation can help to stabilize the ion-pair character product complex; such an effect has been observed widely for many reactions that involve heterolytic cleavage of chemical bond(s).[5b,11,18] In fact, for *p*MP, due to the one-sided solvation configuration, the solvation of the leaving group supplies the *sole* driving force to promote the triplet cleavage. This provides an interpretation for the experimentally observed faster triplet decay of MPPP in $CF_3CH(OH)CF_3$ than in H_2O/CH_3CN or CF_3CH_2OH solvents (Figure 5), since the former solvent has a stronger ability in solvating an anion than the latter solvents. More importantly, this predicts a *critical* dependence of the *p*MP triplet cleavage upon the lability of the leaving group, which is consistent with the experimental observation that, with a better leaving group, the MPPP triplet undergoes fairy efficient cleavage, in sharp contrast to the minor reactivity displayed by the MPEP triplet under the same experimental conditions (Figures 8).

Solvent Dependent Deprotection Mechanism of MPPP and MPEP. Using all of the experimental and calculated results reported here in conjunction with relevant results reported in

---

[18] (a) Newcomb, M.; Horner, J. H.; Whitted, P. O.; Crich, D.; Huang, X. H.; Yao, Q. W.; Zipse, H. *J. Am. Chem. Soc.* **1999**, *121*, 10685–10694. (b) Whitted, P. O.; Horner, J. H.; Newcomb, M.; Huang, X. H.; Crich, D. *Org. Lett.* **1999**, *1*, 153–156. (c) Horner, J. H.; Taxil, E.; Newcomb, M. *J. Am. Chem. Soc.* **2002**, *124*, 5402–5410. (d) Cameron, J. F.; Willson, C. G.; Frechet, J. M. J. *J. Am. Chem. Soc.* **1996**, *118*, 12925–12937. (e) Lipson, M.; Deniz, A. A.; Peters, K. S. *J. Am. Chem. Soc.* **1996**, *118*, 2992–2997.

SCHEME 2

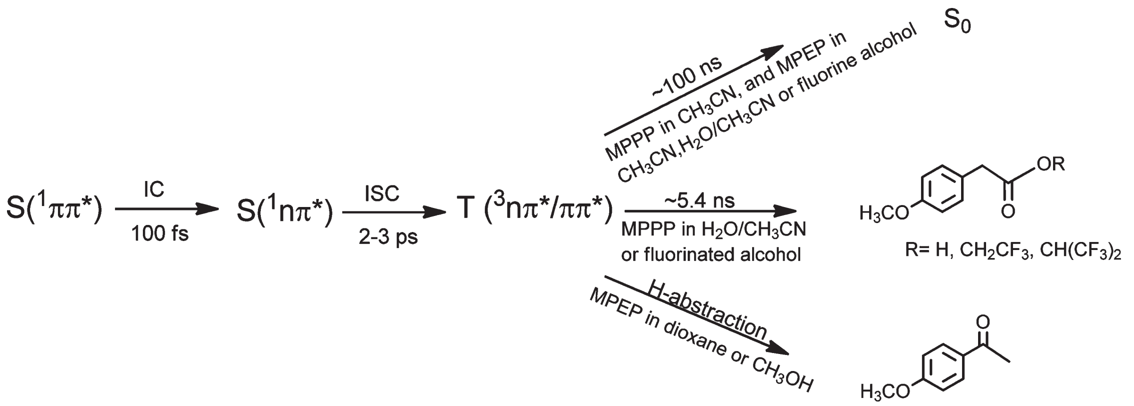

the literature for some closely related systems, the following picture can be developed for the photophysical and photochemical reactions for 267 nm excited MPEP and MPPP. After photoexcitation into the strongly absorbing $^1\pi\pi^*$ state, the system evolves promptly (100 fs) by IC to the energetically nearby ^{1}nπ^* state that is followed by rapid ISC ($\tau \approx 2-3$ ps) into a ^{3}nπ^*/$\pi\pi^*$ mixed character triplet (Scheme 2) that is present in a solvent associated form and acts as the reactive precursor to the subsequent solvent and leaving group dependent chemical reactions. The triplet state is subject to several dynamically competing decay channels. Besides the illustrated heterolytic cleavage (path i) that gives the deprotection and solvolytic rearrangement product (**3** in eq 3), the triplet also has an intrinsic reactivity to perform a H-abstraction owing to the involvement of the ^{3}nπ^* electronic character of the triplet configuration.[7,9,19] The H-abstraction (with a typical rate of $\sim 10^6-10^9$ s^{-1}) may initiate a series of radical processes that can lead to a second deprotection channel (path ii) which is accompanied by formation of the reductive byproduct **2** (eq 3). Of course, other generally involved triplet deactivation channels such as an oxygen quenching (path iii, with a typical rate of $\sim 10^8-10^9$ M^{-1} s^{-1}) that leads to recovery of S$_0$[9] will also contribute to the experimentally observed decay of the triplet.

The actual fate and outcome of the triplet decay is governed by the relative efficiency of these processes, which is in turn affected strongly by the properties of solvent and lability of the leaving group as demonstrated in this work. Like the case of MPPP in the H$_2$O/CH$_3$CN mixed solvent and in the fluorinated alcohols, for the direct heterolytic deprotection to be the predominant triplet decay channel, the system needs to meet a combined requirement of having a good leaving group and use a solvent with strong solvating capability. To include the indirect reductive H-abstraction initiated deprotection, the system needs to use a solvent that is able to donate a H atom. The reductive deprotection reported for MPEP in solvents such as dioxane[2b,c] or methanol[6a,b] provide examples for this. In cases where there is an inert solvent (with little ability in solvating the ion or donating a H atom) used (MPPP in CH$_3$CN for instance) or with an unfavorable leaving group and in a non-H-donating solvent (such as MPEP in CH$_3$CN and H$_2$O/CH$_3$CN and fluorinated alcohols), neither pathway i nor ii could occur appreciably and consequently the oxygen quenching will turn out to be the prevailing channel to deactivate the triplet. This perception of the triplet reaction channel (Scheme 2) provides a unified picture for understanding the overall mechanism and the factors that may affect the pathway and reactivity of the *p*MP triplet.

The reaction mechanisms in Scheme 2 are based on our experiments and previous reports.[2b,c,6a,b] Our TA and TR^3 experimental results provide the first determination of the time constants for the elementary steps involved in the overall deprotection reaction. It is noted that Givens offered a similar photorearrangement reaction mechanism of *p*MP compounds in methanol and *tert*-butyl alcohol that involved a spiroketone species as an intermediate;[6a,b] however, our experimental results show apparently correlated time constants between the decay of the MPPP triplet (~5.4 ns) and the growth of the photorearrangement product (< 10 ns) with little observation of the involvement of any intermediate. This seems to suggest a concerted triplet deprotection and solvolytic rearrangement reactions of MPPP in aqueous solution and fluorinated alcohols.

Comparison of the Triplet Deprotection Mechanisms of *p*MP with *p*HP. Comparison of the deprotection mechanisms proposed for *p*MP and that reported for *p*HP[2,5,16,17,20] reveals some similarities and differences. The major similarities are about the spectral features and the dynamics of the involved photophysical processes that occur before the triplet reaction. This includes the common feature of a very rapid IC, ISC, and the accompanying early time relaxation processes including the excess energy relaxation and solvation related solvent reorganization. The close resemblance of the corresponding TRF, TA, and TR^3 spectra recorded for *p*MP and *p*HP suggests that the corresponding states ($^1\pi\pi^*$, ^{1}nπ^*, and ^{3}nπ^*/$\pi\pi^*$) of the two classes of compounds have generally similar electronic and structural properties. This is well within expectation since the hydroxyl and methoxy groups have similar electronic effects on the intrinsic properties of the electronic states. The differences in the deprotection mechanisms are manifested in two aspects. The first is that unlike the single rearrangement associated deprotection

---

[19] (a) Du, Y.; Ma, C. S.; Kwok, W. M.; Xue, J. D.; Phillips, D. L. *J. Org. Chem.* **2007**, *72*, 7148–7156. (b) Wagner, P. J.; Kemppain., Ae; Schott, H. N. *J. Am. Chem. Soc.* **1973**, *95*, 5604–5614. (c) Wagner, P. J.; Truman, R. J.; Scaiano, J. C. *J. Am. Chem. Soc.* **1985**, *107*, 7093–7097. (d) Wagner, P. J.; Nakahira, T. *J. Am. Chem. Soc.* **1973**, *95*, 8474–8475. (e) Das, P. K.; Encinas, M. V.; Scaiano, J. C. *J. Am. Chem. Soc.* **1981**, *103*, 4154–4162. (f) Scaiano, J. C. *J. Am. Chem. Soc.* **1980**, *102*, 7747–7753.

[20] Givens, R. S.; Heger, D.; Hellrung, B.; Kamdzhilov, Y.; Mac, M.; Conrad, P. G.; Cope, E.; Lee, J. I.; Mata-Segreda, J. F.; Schowen, R. L.; Wirz, J. *J. Am. Chem. Soc.* **2008**, *130*, 3307–3309.

generally displayed by the *p*HP triplet, the triplet of *p*MP shows dual reactivity that can give both the rearrangement and the reductive associated deprotection pathways. Relevant to this is the fact that the occurrence of the *p*MP rearrangement related deprotection requires a much stricter condition and when it happens, it takes place at a much slower rate than the corresponding system of *p*HP. The second aspect is that previous studies on the *p*HP deprotection have established a stepwise deprotection−rearrangement mechanism; the results here on *p*MP appear to suggest that the corresponding reaction of *p*MP is an essentially concerted process without an apparent clear separation.

The cause of the first aspect is related to the methoxy versus hydroxyl substitution and can be connected with the different solvation effects observed for the two kinds of systems. The two-sided solvation adopted in the *p*HP triplet allows for a strong electronic coupling between the triplet and the surrounding water molecules (or other protic solvent molecules). This coupling enables the water molecules to exert a cooperative interaction of both the electronic "push" through solvation of the hydroxyl hydrogen and the electronic "pull" through solvation of the leaving group on the triplet. This concerted operation of these two forces favors strongly the heterolytic cleavage pathway and accounts for the exclusive high efficiency of this pathway relative to the other decay channels. However, in the case of the triplet of *p*MP, the one-sided solvation allows only the "pull" interaction to be built up significantly so the lack of the electronic "push" may be responsible for the relatively higher barrier and the reduced reaction rate of the triplet cleavage in the *p*MP systems. The slow dynamics suppresses the efficiency of this pathway and leads to other channels (H-abstraction, oxygen quenching) to become involved to compete in the deactivation of the triplet. Owing to the general low efficiency, the overall deprotection yield of the *p*MP triplet is much lower than that of the *p*HP triplet.

As to the second aspect, early work on the *p*HP deprotection have found a sequential deprotection and rearrangement pathway T → M → HPAA that involves a transient species M to mediate the phenacyl to phenylacetate solvolytic rearrangement.[1,2d,f−h,3b,4,5b,20] Several species, such as the triplet biradical character *p*-methide quinine (QM)[2f,4,20] and the solvent associated ion character triplet,[2g,5b] have been proposed to help making an assignment to the intermediate M. It is notable that, although further explicit evidence is still needed to differentiate and justify the validity of these species, the species were suggested on the basis of a common consideration, which is the distinct proton-donating capacity of the hydroxyl group in regard to its marked enhanced acidity or deprotonation capacity in the triplet compared to the S_0 state.[2f,5b,13d,21] On this basis, the hydroxyl group has been taken as being crucially important in determining the reactivity and the stepwise pathway of the *p*HP deprotection and solvolytic rearrangement processes. The currently observed apparently concerted deprotection−rearrangement of the MPPP triplet implies that while the hydroxyl group is not totally necessary for the deprotection to take place, the hydroxyl group may act to contribute a favorable factor to facilitate lowering the free energy barrier of the deprotection reaction so as to make it faster. To the best of our knowledge, our observation of the close to concerted deprotection and rearrangement for MPPP presents the first direct monitoring of reactions of this type. In summary, the different reaction pathways exhibited by the *p*MP and *p*HP triplets adds a new example for the versatile reactivity of the triplets of aromatic carbonyl compounds. The results here demonstrate that the substituent group and solvent properties play an important part in modifying the reaction pathways and determining the photoproduct distribution.

Conclusion

Femtosecond time-resolved fluorescence (fs-TRF), femtosecond transient absorption (fs-TA), and picosecond and nanosecond time-resolved Raman (ps-, ns-TR^3) experiments were conducted to study the kinetics and mechanisms of the photodeprotection and rearrangement reactions for the *p*MP compounds *p*-methoxyphenacyl diethyl phosphate (MPEP) and diphenyl phosphate (MPPP) in acetonitrile, in water/acetonitrile mixed solvents, and in fluorinated alcohol solvents. The results reported here show that rapid IC (100 fs) and ISC (~2−3 ps) processes lead to a $^3n\pi^*/\pi\pi^*$ mixed character triplet after 267 nm photoexcitation. The triplet is present in a solvent associated form and acts as the reactive precursor to the subsequent solvent and leaving group dependent chemical reactions seen in the experimental data. The DFT calculation results provide a theoretical explanation for the effect of the methoxy versus hydroxyl substitution on the triplet reactivity and indicate that the solvent and lability of the leaving group play a crucial role in determining the rate and pathways of the triplet deprotection. The one-sided leaving group solvation configuration observed for *p*MP triplets in the water-containing solvents is responsible for the modest triplet heterolytic deprotection that also gives some rearrangement product. This combined with the $n\pi^*/\pi\pi^*$ character of the *p*MP triplets helps to interpret the inclusion of the alternative reduction associated deprotection pathway exhibited by *p*MP in some hydrogen-donating solvents.

Experimental and Computational Methods

MPEP and MPPP were prepared following the methods previously described in the literature.[2b,e] The identity and purity of these prepared compounds were confirmed by analysis of the MS, NMR, and UV−vis absorption spectra. Details of the preparation and characterization of these compounds are given in the Supporting Information. The solution samples used for the time-resolved and steady-state measurements described in this work were prepared using commercial organic solvents (HPLC-grade CH_3CN and GC grade (≥99%) for others) and deionized water.

The apparatus and methods used for the fs-TA, fs-TRF, and ps-TR^3 experiments were described previously.[5] Briefly, the third harmonic (267 nm) and fundamental laser pulses (800 nm) from a commercial Ti:Sapphire regenerative amplifier laser system were used as pump and probe laser pulses in the TA experiment. The time resolution of the TA measurement was about 200 fs. The spot sizes of the pump and probe beams at the sample were about 200 and 100 μm, respectively.[5b] The same Ti:Sapphire regenerative amplifier laser system was employed in the TRF experiments with a 150 fs pulse duration and 1 kHz repetition rate as the excitation and gating pulses, respectively. The excitation pulses (~0.5 μJ) were focused (~100 μm) into a 0.5 mm thick jet stream of sample placed at one focus of an ellipsoidal mirror.[5a] For the ps-TR^3 measurements, the third

---

(21) (a) Huck, L. A.; Wan, P. *Org. Lett.* **2004**, *6*, 1797–1799. (b) Tolbert, L. M.; Haubrich, J. E. *J. Am. Chem. Soc.* **1994**, *116*, 10593–10600. (c) Webb, S. P.; Yeh, S. W.; Philips, L. A.; Tolbert, M. A.; Clark, J. H. *J. Am. Chem. Soc.* **1984**, *106*, 7286–7288.

harmonic (267 nm) and the second harmonic (400 nm) from the Ti:Sapphire regenerative amplifier laser system with ~1.5 ps pulse duration and 1 kHz output were utilized as pump and probe laser pulses. The pump and probe beams were set at the magic angle and focused to ~200 μm spot size on the sample with pulse energies of 2−3 μJ.[5] The apparatus and methods employed for the ns-TR^3 experiments have been described previously,[12,13] and only a short description will be provided here. The harmonics and/or their hydrogen Raman shifted laser lines from two nanosecond Nd:YAG laser systems supplied the pump (266 nm) and probe (223 or 416 nm) wavelengths used in the ns-TR^3 experiments, and a near colinear geometry was employed to focus them onto a flowing liquid stream of sample. The time resolution of the experiments was approximately 5−10 ns. The signals for all the experiments were collected and detected by a nitrogen-cooled CCD detector, and then the data were sent to an interfaced PC computer. Sample solutions for these experiments were typically at 1−1.5 mM concentration.

The photochemistry of the reactions for MPPP in H_2O/CH_3CN and in CF_3CH_2OH were monitored by measuring the UV−vis absorption spectrum of the sample solution (~0.1 mM concentration) before and after exposure to an unfocused 266 nm laser line (~3.5 mJ) from the fourth harmonic of a nanosecond Nd:YAG Q-switch laser. The sample solution was put in a 1 cm UV grade cell and excited by the 267 nm laser beam. As the reaction progressed, the UV−vis absorption spectrum of the photolyzed sample was measured by using a Perkin-Elmer Lambda 19 UV−vis spectrometer.

The reactant, product, and transition state geometries for the MPPP triplet deprotection with the involvement of explicit solvent water molecules were optimized at the (U)B3LYP/6-31G* level of theory using the Gaussian 03 program suite.[22] Vibrational frequency calculations were performed for all of the stationary points in order to obtain corrections for the zero point energies (ZPEs) and to ensure that the computed reactant and product are the corresponding local minimum and the transition states were first-order saddle points. Intrinsic reaction coordination (IRC) computations[23] were done to confirm that the transition states connected the corresponding reactants and products. The Cartesian coordinates, the total energies, and selected output from the calculations for the precursor species, intermediates, transition states, and final byproduct are provided in the Supporting Information. Additional calculations using the 6-311+G(d, p) basis set were done for the for HPEP and MPEP reactions, and these results were compared to the results from the calculations already done for the 6-31G* basis set (see Table 3S in the Supporting Information). The results for HPEP and MPEP found that the free energy differences from using the 6-311+G(d,p) basis set are both similar to the corresponding ones obtained from the 6-31G* set and suggest that the data from 6-31G* may be useful to gain some insight into the reactions examined here.

Acknowledgment. The research was supported by grants from the Research Grants Council of Hong Kong (HKU 1/01C and HKU 7039/07P) to D.L.P. and (PolyU/7029/07p and PolyU/5007/08p) to W.M.K. D.L.P. thanks the Croucher Foundation for the Award of a Senior Research Fellowship and the University of Hong Kong for the Outstanding Researcher Award.

Supporting Information Available: Recorded spectra of the MPPP photochemistry experiments in the H_2O/CH_3CN (1:1, v/v) mixed solvent and in the CF_3CH_2OH solvent; fs-TA spectra of MPPP in CF_3CH_2OH and the fs-TA spectra acquired for *p*-methoxyacetophenone in neat MeCN and MeCN/H_2O; ns-TR^3 spectra obtained for MPEP and MPPP in CF_3CH_2OH obtained with 266 nm pump and 416 nm (ns-TR^3) probe wavelengths at various delay times; time dependences of the MPEP and MPPP triplets in CF_3CH_2OH; ns-TR^3 spectra of MPPP in CF_3CH_2OH obtained with 266 nm pump and 223 nm probe wavelengths at various delay times; time dependence of MPPP in CF_3CH_2OH; key geometry information of the HPEP and MPEP reactant complexes (RC) and transition states (TS) obtained at the (U)B3LYP/6-31G* level of theory for the C and O atoms where the cleavage occurs in the deprotection reaction; Cartesian coordinates, total energies, and vibrational zero-point energies determined for the optimized geometries of the HPEP, HPPP, MPEP and MPPP complexes with four water molecules. This material is available free of charge via the Internet at http://pubs.acs.org.

---

[22] Frisch, M. J.; Trucks, G. W.; Schlegel, H. B.; Scuseria, G. E.; Robb, M. A.; Cheeseman, J. R.; Zakrzewski, V. G.; Montgomery, J. A. J.; Stratmann, R. E.; Burant, J. C.; Dapprich, S.; Millam, J. M.; Daniels, A. D.; Kudin, K. N.; Strain, M. C.; Farkas, O.; Tomasi, J.; Barone, V.; Cossi, M.; Cammi, R.; Mennucci, B.; Pomelli, C.; Adamo, C.; Clifford, S.; Ochterski, J.; Petersson, G. A.; Ayala, P. Y.; Cui, Q.; Morokuma, K.; Malick, D. K.; Rabuck, A. D.; Raghavachari, K.; Foresman, J. B.; Cioslowski, J.; Ortiz, J. V.; Baboul, A. G.; Stefanov, B. B.; Liu, G.; Liashenko, A.; Piskorz, P.; Komaromi, I.; Gomperts, R.; Martin, R. L.; Fox, D. J.; Keith, T.; Al-Laham, M. A.; Peng, C. Y.; Nanayakkara, A.; Gonzalez, C.; Challacombe, M.; Gill, P. M. W.; Johnson, B.; Chen, W.; Wong, M. W.; Andres, J. L.; Gonzalez, C.; Head-Gordon, M.; Replogle, E. S.; Pople, J. A. *Gaussian 98, revision A.7*; *Gaussian 03s, revision B.05*; Gaussian Inc.: Pittsburgh, PA, 1998, 2003.

[23] (a) Gonzalez, C.; Schlegel, H. B. *J. Chem. Phys.* **1989**, *90*, 2154–2161. (b) Gonzalez, C.; Schlegel, H. B. *J. Phys. Chem.* **1990**, *94*, 5523–5527.